Estrogen promotes the survival and pulmonary metastasis of tuberin-null cells

Jane J. Yu[a,1], Victoria A. Robb[a], Tasha A. Morrison[a], Eric A. Ariazi[a], Magdalena Karbowniczek[a], Aristotelis Astrinidis[b], Chunrong Wang[a], Lisa Hernandez-Cuebas[b], Laura F. Seeholzer[a], Emmanuelle Nicolas[a], Harvey Hensley[a], V. Craig Jordan[a], Cheryl L. Walker[c], and Elizabeth P. Henske[a,d,1]

[a]Fox Chase Cancer Center, Philadelphia, PA 19111; [b]Drexel University College of Medicine, Philadelphia, PA 19102; [c]University of Texas, M. D. Anderson Cancer Center, Smithville, TX 78957; and [d]Brigham and Women's Hospital and Harvard Medical School, Boston, MA 02115

Edited by Melanie H. Cobb, University of Texas Southwestern Medical Center, Dallas, TX, and approved December 16, 2008 (received for review October 24, 2008)

Lymphangioleiomyomatosis (LAM) is an often fatal disease primarily affecting young women in which tuberin (TSC2)-null cells metastasize to the lungs. The mechanisms underlying the striking female predominance of LAM are unknown. We report here that 17-β-estradiol (E_2) causes a 3- to 5-fold increase in pulmonary metastases in male and female mice, respectively, and a striking increase in circulating tumor cells in mice bearing tuberin-null xenograft tumors. E_2-induced metastasis is associated with activation of p42/44 MAPK and is completely inhibited by treatment with the MEK1/2 inhibitor, CI-1040. In vitro, E_2 inhibits anoikis of tuberin-null cells. Finally, using a bioluminescence approach, we found that E_2 enhances the survival and lung colonization of intravenously injected tuberin-null cells by 3-fold, which is blocked by treatment with CI-1040. Taken together these results reveal a new model for LAM pathogenesis in which activation of MEK-dependent pathways by E_2 leads to pulmonary metastasis via enhanced survival of detached tuberin-null cells.

anoikis | MAPK | lymphangioleiomyomatosis | Bim | Rheb

LAM, the pulmonary manifestation of tuberous sclerosis complex (TSC), affects women almost exclusively (1). LAM affects 30−40% of women with TSC (2, 3). In a Mayo Clinic series, LAM was the third most frequent cause of TSC-related death, after renal disease and brain tumors (4). LAM can also occur in women who do not have germline mutations in *TSC1* or *TSC2* (sporadic LAM). LAM cells from both TSC-LAM and sporadic LAM carry inactivating mutations in both alleles of the *TSC1* or *TSC2* genes (5). The protein products of *TSC1* and *TSC2*, hamartin and tuberin, respectively, form heterodimers (6, 7) that inhibit the small GTPase *R*as *h*omologue *e*nriched in *b*rain (Rheb), via tuberin's highly conserved GTPase activating domain. In its active form, Rheb activates the mammalian target of rapamycin (mTOR) complex 1 (TORC1), which is a key regulator of protein translation, cell size, and cell proliferation (8). Evidence of TORC1 activation, including hyperphosphorylation of ribosomal protein S6, has been observed in tumor specimens from TSC patients and LAM patients (9–11). Independent of its activation of mTOR, Rheb inhibits the activity of B-Raf and C-Raf/Raf-1 kinase, resulting in reduced phosphorylation of p42/44 MAPK (12–14), but the impact of the Raf/MEK/MAPK pathway on disease pathogenesis is undefined.

LAM is characterized pathologically by widespread proliferation of abnormal smooth muscle cells and by cystic changes within the lung parenchyma (1). About 60% of women with the sporadic form of LAM also have renal angiomyolipomas. The presence of *TSC2* mutations in LAM cells and renal angiomyolipoma cells from women with sporadic LAM, but not in normal tissues, has led to the hypothesis that LAM cells spread to the lungs via a metastatic mechanism, despite the fact that LAM cells have a histologically benign appearance (15, 16). Genetic and fluorescent in situ hybridization analyses of recurrent LAM after lung transplantation support this benign metastatic model (16).

The female predominance of LAM, coupled with the genetic data indicating that LAM cells are metastatic, suggests that estrogen may promote the metastasis of tuberin-null cells. Both LAM cells and angiomyolipoma cells express estrogen receptor alpha (17), and there are reports of symptom mitigation in LAM patients after oophorectomy and worsening of symptoms during pregnancy (1). However, the molecular and cellular mechanisms that may underlie an impact of estrogen on the metastasis of LAM cells are not well defined, in part because of the lack of in vivo models that recapitulate the metastatic behavior of LAM cells.

We report here that estrogen promotes the pulmonary metastasis of Tsc2-null ELT3 cells. This enhanced metastasis is associated with elevated levels of circulating tumor cells and with activation of p42/44 MAPK. When Tsc2-null cells are injected intravenously, E_2 enhances their survival and lung colonization, and in vitro, E_2 inhibits anoikis of Tsc2-null cells. In vivo, the MEK inhibitor CI-1040 blocks E_2-induced lung metastasis, decreases circulating tumor cells, and reduces lung colonization. Taken together, these data reveal that the MEK pathway is a critical component of the estrogen-dependent metastatic potential of Tsc2-null cells and lead to a unique model of LAM pathogenesis with therapeutic implications in which E_2 promotes the survival of disseminated LAM cells, thereby facilitating lung colonization and metastasis.

Results

Estrogen Promotes the Pulmonary Metastasis of Tuberin-Deficient ELT3 Cells in Ovariectomized Female Mice and in Male Mice. To study the role of E_2 in the metastasis of Tsc2-null cells, we used ELT3 cells, which were originally derived from a uterine leiomyoma in the Eker rat model of Tsc2 and, similar to LAM cells, express smooth muscle cell markers and estrogen receptor alpha (18, 19). To confirm that ELT3 cells proliferate in response to estrogen stimulation in vitro, cell growth was measured using ^{3}H-thymidine incorporation. E_2 treatment resulted in a significant increase in ^{3}H-thymidine incorporation by 2.8-fold on day 5 ($P = 0.03$, Fig. 1*A*), similar to the findings of Howe *et al.* (19).

ELT3 cells were inoculated s.c. into the flanks of ovariectomized CB17-*SCID* mice, which were supplemented 1 week before with either placebo or E_2 pellets (2.5 mg, 90-day release). Tumors arose in 100% of both estrogen and placebo-treated mice. At postinoculation week 8, estrogen-treated mice had a mean tumor area

Author contributions: J.J.Y. and E.P.H. designed research; J.J.Y., T.A.M., M.K., A.A., C.W., L.H.-C., L.F.S., and E.N. performed research; E.A., H.H., V.C.J., and C.L.W. contributed new reagents/analytic tools; J.J.Y. analyzed data; and J.J.Y., V.A.R., and E.P.H. wrote the paper.

The authors declare no conflict of interest.

This article is a PNAS Direct Submission.

Freely available online through the PNAS open access option.

[1]To whom correspondence may be addressed. E-mail: jyu13@partners.org or ehenske@partners.org.

This article contains supporting information online at www.pnas.org/cgi/content/full/0810790106/DCSupplemental.

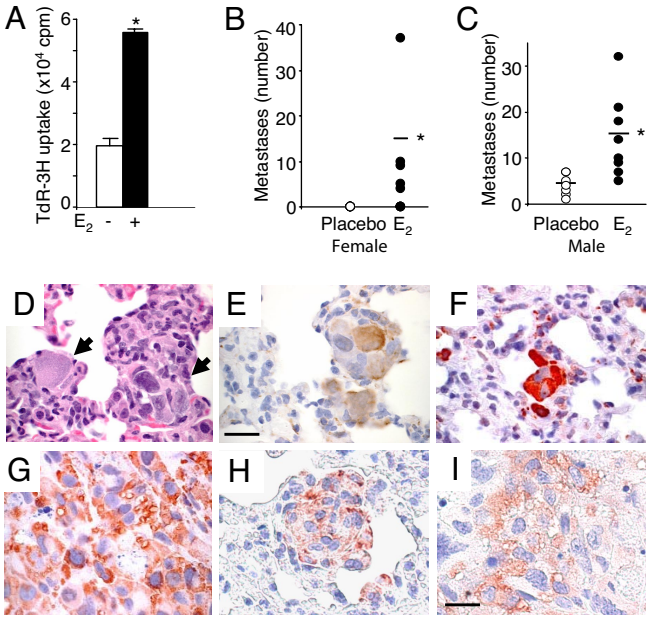

Fig. 1. Estrogen promotes the lung metastasis of tuberin-deficient ELT3 cells in female and male mice. (*A*) The proliferation of ELT3 cells in response to E_2 was measured by ^{3}H-thymidine incorporation after 5 days of growth. (*B–J*) ELT3 cells were injected s.c. into the flanks of female ovariectomized and male *SCID* mice implanted with E_2 ($n = 9$) or placebo ($n = 10$) pellets. (*B*) Lung metastases were scored from E_2 ($n = 9$) or placebo-treated ($n = 10$) mice. (*C*) The number of lung metastases in male mice was scored from placebo ($n = 10$) and E_2-treated ($n = 9$) mice. (*D–I*) Consecutive lung sections containing metastases (arrows) from an E_2-treated female mouse were stained with H&E (*D*), anti-smooth muscle actin (*E*), and anti-phospho-S6 (*F*). (Scale bar, 50 μM.) (*G*) Anti-phospho-S6 immunostain of the primary xenograft tumor of an estrogen-treated female mouse. (*H* and *I*) Phospho-S6 immunoreactivity of a metastasis (*H*) and xenograft tumor (*I*) of an estrogen-treated male mouse. (Scale bar, 20 μM.) *, $P < 0.05$, Student's *t* test.

of 287 ± 43 mm^2, whereas placebo-treated mice had a mean tumor area of 130 ± 20 mm^2 ($P = 0.0035$), consistent with previous findings (19). The proliferative potential of ELT3 cells in vivo was examined using Ki-67 immunoreactivity. The number of Ki-67 positive cells in estrogen-treated tumors was 17% higher than the number in placebo-treated tumors ($P = 0.03$).

Pulmonary metastases were identified in 5 of 9 E_2-treated mice (56%), with an average of 15 metastases/mouse (range 4–37) (Fig. 1*B*). In contrast, only 1 of 9 placebo-treated mice (10%) developed a single metastasis ($P = 0.039$). To determine whether the enhanced metastasis was directly related to tumor size, a subset of placebo-treated mice ($n = 4$) and estrogen-treated mice ($n = 4$) that developed primary tumors at similar size (209 ± 16 and 198 ± 20 mm^2, respectively) was analyzed separately. Three of the estrogen-treated mice developed pulmonary metastases with an average of 6 metastases/mouse, while none of the placebo-treated mice developed metastases.

Next, we inoculated ELT3 cells into male mice. At 8 weeks post-cell inoculation, E_2-treated animals developed tumors that were 2.9-fold larger than those in the placebo-treated animals. As in the female mice, E_2 significantly enhanced the frequency and the number of pulmonary metastases. At 8 weeks post-inoculation, 10 of 10 (100%) of the E_2-treated mice developed metastases, with an average of 14 metastases/mouse (range 5–32). In contrast, 7 of 10 (70%) of the placebo-treated mice developed metastases, with an average of 4 metastases/mouse (range 1–7, $P = 0.013$) (Fig. 1*C*). As expected, the metastatic and primary tumor cells were immunoreactive for smooth muscle actin and phospho-ribosomal protein S6 (Fig. 1 *D–I*).

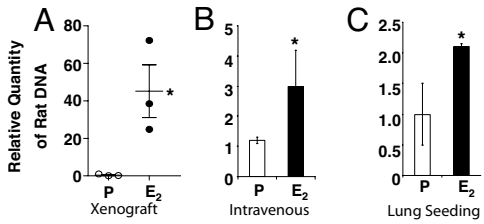

Fig. 2. Estrogen increases circulating tumor cells in mice bearing xenograft tumors and enhances the survival and lung seeding of intravenously injected Tsc2-null cells. (*A*) DNA prepared from the blood of placebo ($n = 3$) and E_2-treated ($n = 3$) mice bearing xenograft tumors of similar size (≈1,000 mm^3) was analyzed by real-time PCR using rat-specific primers to quantitate circulating tumor cells. (*B*) Levels of circulating tumor cell DNA 6 h after i.v. injection of ELT3 cells into placebo ($n = 3$) and E_2-treated ($n = 3$) mice. (*C*) Levels of tumor cell DNA in the lungs 24 h after i.v. injection of ELT3 cells into placebo ($n = 3$) and E_2-treated ($n = 3$) mice. *, $P < 0.05$, Student's *t* test.

Estrogen Increases Circulating Tumor Cell DNA. To determine whether the mechanism of E_2-driven metastasis of ELT3 cells is associated with an increase in survival of ELT3 cells in the circulation, we analyzed blood collected from xenograft mice at 7 weeks post-cell inoculation. Real-time PCR with rat-specific primers was used to measure the relative quantity of tumor cells circulating in the blood. We selected 6 animals (3 placebo, 3 E_2-treated) bearing tumors of similar size (≈1,000 mm^3) for this analysis. The E_2-treated animals had a striking increase in the amount of circulating tumor cell DNA as compared to that in the placebo-treated animals ($P = 0.034$, Fig. 2*A*).

This increased level of circulating tumor cell DNA suggested that E_2 may promote the survival of Tsc2-null cells upon dissemination from the primary tumor site. To test this, we injected 2×10^5 ELT3 cells intravenously and again measured the amount of tumor cell DNA using real-time PCR. E_2 treatment resulted in a 2.5-fold increase in circulating cells 6 h post-injection ($P = 0.047$, Fig. 2*B*). To determine whether this enhanced survival of circulating cells was associated with increased colonization of the lungs, the mice were killed 24 h after injection, and the lungs were analyzed by real-time PCR. E_2 treated mice had a 2-fold increase in the lung seeding of ELT3 cells ($P = 0.039$, Fig. 2*C*).

Estrogen Promotes the Lung Colonization of ELT3 Cells in Vivo. To identify the earliest time points at which estrogen exerts an effect on the survival of intravenously injected Tsc2-null cells, ELT3 cells that stably express luciferase (ELT3-Luc) were intravenously injected. The level of bioluminescence was evaluated using the Xenogen IVIS System. At 1 h post-cell injection, similar levels of bioluminescence were observed in the chest regions of E_2 and placebo-treated mice. By 3 h, the bioluminescence in the chest regions was 2-fold higher in the E_2-treated animals than in the placebo-treated animals, and at 24 h post-cell injection it was 5-fold higher in the E_2-treated animals ($P = 0.043$, Fig. 3 *A* and *B*). After sacrifice, the lungs were dissected and imaged in Petri dishes to confirm that the bioluminescent signals in the chest regions of the living mice were a result of lung colonization (Fig. 3*C*).

Estrogen Activates p42/44 MAPK in ELT3 Cells in Vitro and in Vivo. These results suggested that E_2 promotes the survival of disseminated ELT3 cells. To determine the mechanism of this, we focused on the Raf/MEK/MAPK signaling cascade. This pathway is inhibited in cells lacking TSC2 via Rheb's inhibition of B-Raf and C-Raf/Raf-1 kinase (13, 14). E_2 has been shown to activate p42/44 MAPK in ELT3 cells and in LAM patient-derived cells (11, 20, 21). To confirm that E_2 activates MAPK in ELT3 cells, we treated the cells with 10 nM E_2 and examined the phosphorylation status of p42/44 MAPK by immunoblotting. Within 15 min, E_2 induced the phosphorylation of p42/44 MAPK (Fig. 4*A*). We also found that

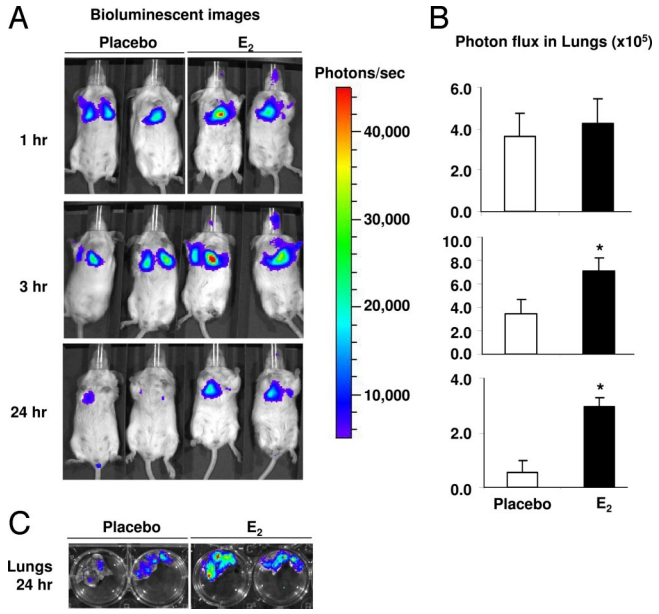

Fig. 3. Estrogen promotes the lung colonization of Tsc2-null ELT3 cells. (*A*) ELT3-luciferase cells were injected intravenously into ovariectomized female placebo ($n = 3$) and E_2-treated ($n = 3$) mice. Lung colonization was measured using bioluminescence at 1, 3, and 24 h after injection. Representative images are shown. (*B*) Total photon flux/second present in the chest regions in placebo ($n = 3$) and E_2-treated ($n = 3$) animals. *, $P < 0.05$, Student's *t* test. (*C*) Lungs were dissected 24 h postcell injection and bioluminescence was imaged in Petri dishes.

E_2-induced phosphorylation of p42/44 MAPK was blocked by the MEK1/2 inhibitor PD98059 (Fig. 4*A*), which is in contrast to the prior work of Finlay *et al.* (20). E_2 is known to rapidly activate C-Raf (22). We hypothesized that E_2 reactivates MAPK via a Rheb-independent pathway in cells lacking tuberin. In a separate experiment, we found that E_2 rapidly (within 2 min) increased the phosphorylation of C-Raf at Ser-338, a site which is closely linked with C-Raf activity (Fig. 4*B*). However, E_2 does not affect mTOR activation as measured by ribosomal protein S6 phosphorylation (Fig. 4*C*). These results suggest that E_2 does not regulate Rheb activity and that the potential of E_2 to impact the Raf/MEK/ERK kinase cascade is Rheb independent. Nuclear translocation of phospho-MAPK was observed within 5 min of E_2 exposure (Fig. 4*D*).

These in vitro findings led us to examine whether E_2 activates p42/44 MAPK in ELT3 cells in vivo. In lungs from E_2-treated animals, nuclear phospho-p42/44 MAPK staining was observed in metastases but not in adjacent normal tissues (Fig. 4 *E* and *F*). In the primary xenograft tumors, the percentage of cells with primarily nuclear phospho-MAPK was significantly higher in the tumors from the E_2-treated animals, compared to the tumors from placebo-treated animals (65% vs. 28%, $P = 0.001$, Fig. 4 *G–I*).

Estrogen Increases the Resistance of ELT3 Cells to Anoikis in Vitro. These in vivo findings suggest that estrogen enhances the survival of circulating tumor cells in a MAPK-dependent manner. Because detached cells normally undergo apoptosis (23–25), a critical first step in cancer progression is the development of resistance to matrix deprivation-induced apoptosis (anoikis) (26, 27). Therefore, to investigate the mechanism of E_2-prolonged survival of ELT3 cells in the circulation, we examined the effect of estrogen on anoikis. ELT3 cells were treated for 24 h with either 10 nM E_2 or control and then plated onto PolyHEMA, which prevents attachment and therefore induces anoikis. Cell lysates were immunoblotted for cleaved caspase-3, which is a measure of apoptosis. E_2 treatment reduced caspase-3 cleavage at 6, 16, and 24 h (Fig. 5*A*). E_2 treatment also significantly reduced DNA fragmentation at 1 and 24 h ($P =$

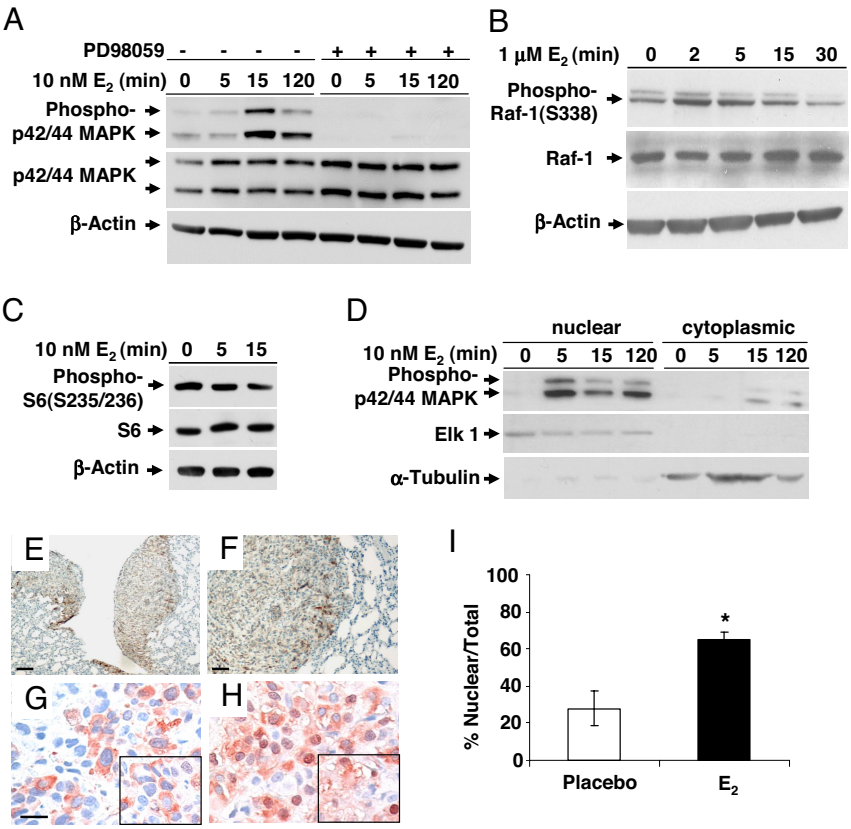

Fig. 4. Estrogen activates p42/44 MAPK in ELT3 cells in vitro and in vivo. (*A*) ELT3 cells were grown in phenol red-free and serum-free media for 24 h and then stimulated with 10 nM E_2 for 0, 5, 15, or 120 min. Levels of phosphorylated p42/44 MAPK and total MAPK were determined by immunoblot analysis. Pretreatment with PD98059 blocked E_2-induced MAPK activation. β-Actin immunoblotting was included as a loading control. (*B*) Levels of phosphorylated C-Raf/Raf-1 and total Raf-1 after E_2 stimulation. (*C*) Levels of phosphorylated S6 after E_2 stimulation. (*D*) The nuclear and cytoplasmic fractions were separated, and levels of phospho-p42/44 MAPK were examined by immunoblot analysis. Anti-ELK1 and anti-α-tubulin were included as loading controls for the nuclear and cytosolic fractions, respectively. (*E* and *F*) Pulmonary metastases from an E_2-treated mouse showed hyperphosphorylation of p42/44 MAPK. (Scale bar, 50 μM and 125 μM.) (*G* and *H*) Phospho-p42/44 MAPK (T202/Y204) immunostaining of primary tumor sections from placebo-treated (*G*) and E_2-treated (*H*) mice. (Scale bar, 20 μM.) (*I*) Percentage of cells with nuclear immunoreactivity of phospho-p42/44 MAPK was scored from 4 random fields per section. *, $P < 0.05$, Student's *t* test.

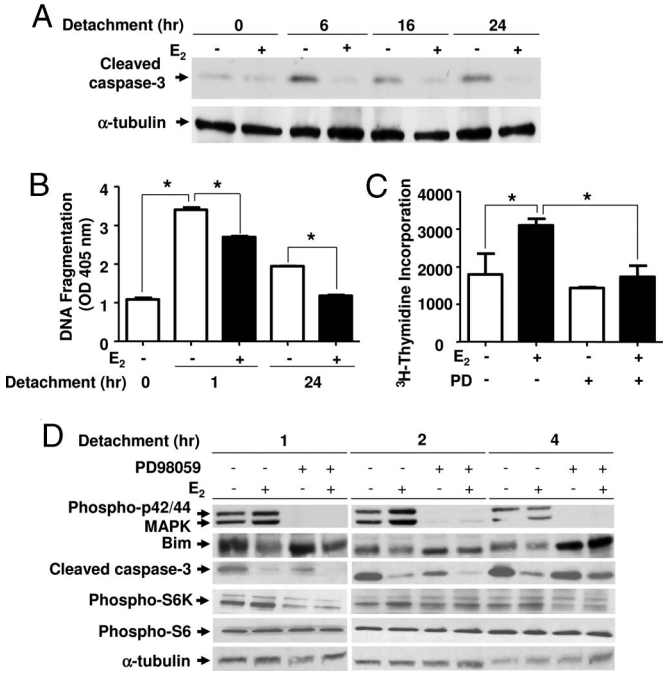

Fig. 5. Estrogen increases the resistance of ELT3 cells to anoikis. ELT3 cells were grown in phenol red-free and serum-free media for 24 h and then treated with 10 nM E_2 for 24 h before culturing on PolyHEMA plates. The MEK1/2 inhibitor PD98059 was begun 15 min before detachment. (*A*) The level of cleaved caspase-3 was determined by immunoblot analysis. α-Tubulin is included as a loading control. (*B*) DNA fragmentation was assessed by ELISA. (*C*) Cell growth was measured by ^{3}H-thymidine incorporation after 24 h of growth on PolyHEMA plates in the presence or absence of E_2, followed by 24 h of growth on adherent plates in the absence of E_2. (*D*) Levels of phospho-p42/44 MAPK, MAPK, Bim, cleaved caspase-3, phospho-S6K, and phospho-S6 were determined by immunoblot analysis. α-Tubulin is included as a loading control. *, $P < 0.05$, Student's *t* test.

0.001 and $P = 0.015$, Fig. 5*B*), which indicates that E_2 inhibits anoikis of Tsc2-null cells.

To confirm further that E_2 promotes the survival of detached cells, ELT3 cells were plated onto PolyHEMA plates for 24 h and replated onto normal tissue culture dishes. Cell growth was measured using ^{3}H-thymidine incorporation. E_2 treatment resulted in a significant increase in ^{3}H-thymidine incorporation 24 h after replating ($P = 0.008$, Figure 5*C*). This E_2-enhanced survival was blocked by treatment with the MEK1/2 inhibitor PD98059 ($P = 0.035$, Fig. 5*C*).

To determine the components that mediate estrogen-enhanced resistance of ELT3 cells to anoikis, we analyzed the proapoptotic protein, Bcl-2 interacting mediator of cell death (Bim), which is known to be a critical activator of anoikis (23). Bim is phosphorylated by protein kinases, including p42/44 MAPK, which leads to rapid proteasomal-mediated degradation and increased cell survival (28). Bim protein level was examined by immunoblotting. We found that estrogen decreased the accumulation of Bim after 1 h in detachment conditions (Fig. 5*D*). Preincubation with the MEK inhibitor PD98059 partially blocked estrogen's inhibition of Bim accumulation and caspase-3 cleavage after 4 h in detachment conditions (Fig. 5*D*). We also examined the phosphorylation of S6K and S6 in detachment conditions and found that the phosphorylation of S6K and S6 did not change with E_2 stimulation. Interestingly, treatment with PD98059 decreased the phosphorylation of S6K 1 h after detachment (Fig. 5*D*).

The MEK1/2 Inhibitor CI-1040 Blocks the Estrogen-Driven Metastasis of ELT3 Cells in Vivo. These in vitro and in vivo results suggest that E_2-induced activation of the MEK/MAPK pathway contributes to the metastatic potential of circulating Tsc2-null ELT3 cells. To determine the effect of inhibiting the MEK/MAPK pathway on the pulmonary metastasis of Tsc2-null cells in vivo, we used the MEK1/2 inhibitor, CI-1040. Beginning 1 day post-subcutaneous inoculation of ELT3 cells, animals, implanted with either placebo or estrogen pellets, were treated with CI-1040 (150 mg/kg day by gavage, twice a day) (29). CI-1040 delayed tumor formation (Fig. 6*A*) and reduced the size of primary tumors by 25% in E_2 animals (Fig. 6*B*), although these data did not reach statistical significance. CI-1040, however, significantly reduced the levels of circulating ELT3 cells in the blood of E_2-treated animals by 84% ($P = 0.042$, Fig. 6*C*). Most strikingly, no lung metastases were detected in mice treated with E_2 plus CI-1040 ($P = 0.046$, Fig. 6 *D* and *E*).

To investigate further the role of MEK/ERK on the survival of ELT3 cells in the circulation, ELT3-luciferase cells were intravenously injected into mice treated with E_2 alone or E_2 plus CI-1040. At 2 h post-cell injection, similar levels of bioluminescence were observed in the chest regions of all mice. At 5 h, the bioluminescence in the chest regions of the E_2 plus CI-1040 treated mice was decreased by 55%, as compared to that in the E_2-treated mice ($P = 0.02$, Fig. 6*F*). After sacrifice at 60 h postcell injection, the bioluminescent signals in the ex vivo lungs of the E_2 plus CI-1040-treated mice were significantly reduced by 96%, as compared to the signals in the E_2-treated animals ($P = 0.0045$, Fig. 6*F*).

Inhibition of mTOR Blocks Estrogen-Induced Pulmonary Metastasis of Tsc2-Null Cells. To determine the role of mTOR signaling pathway in the estrogen-induced metastasis of tuberin-deficient ELT3 cells, the mTORC1 inhibitor RAD001 (4 mg/kg/day by gavage) was administered 5 days per week beginning 1 day post-cell inoculation. RAD001 completely blocked both primary tumor development (Fig. 7*A*) and lung metastasis (Fig. 7*B*) in the presence of estrogen or placebo.

Discussion

LAM is associated with a very unusual disease mechanism: the metastasis of histologically benign TSC1 or TSC2-null cells. LAM has one of the strongest gender predispositions of any extragenital human disease, with a higher female-to-male ratio than even breast cancer. Estrogen receptor alpha is expressed in LAM cells and in angiomyolipoma cells from LAM patients (17), and estrogen has been shown to activate p42/44 MAPK and stimulate the proliferation of Tsc2-null ELT3 cells and TSC2-null angiomyolipoma cells (11). Estrogen has also been shown to enhance liver hemangioma development in Tsc2± mice (30). Despite these findings, the role of estrogen in LAM pathogenesis is not well defined.

We report here that estrogen treatment of both female and male mice bearing Tsc2-null ELT3 xenograft tumors results in an increase in pulmonary metastases. The estrogen-driven metastasis of ELT3 cells was associated with activation of p42/44 MAPK both in vitro and in vivo. Treatment of the mice with the MEK1/2 inhibitor CI-1040 completely blocked the lung metastases in estrogen-treated animals, while causing only a 25% reduction in the size of the primary xenograft tumors, indicating that activation of MEK by E_2 is a critical factor in the metastasis of Tsc2-null cells. In contrast to CI-1040, the mTOR inhibitor RAD001 completely blocked formation of the primary tumor.

Estrogen is known to activate the MAPK pathway (31–34). We speculate that tuberin-null cells may be particularly sensitive to activation of the Raf/MEK/MAPK signaling cascade by estrogen, because at baseline this signaling pathway is inhibited by Rheb, the target of tuberin's GTPase activating protein domain (12–14). Metastasis is a complex process, and there are numerous mechanisms through which estrogen's activation of MEK may enhance the metastasis of Tsc2-null cells. Our in vitro studies revealed that estrogen induces resistance to anoikis in Tsc2-null cells, which suggests that one of these mechanisms involves the survival of detached cells. Consistent with this, we found markedly elevated

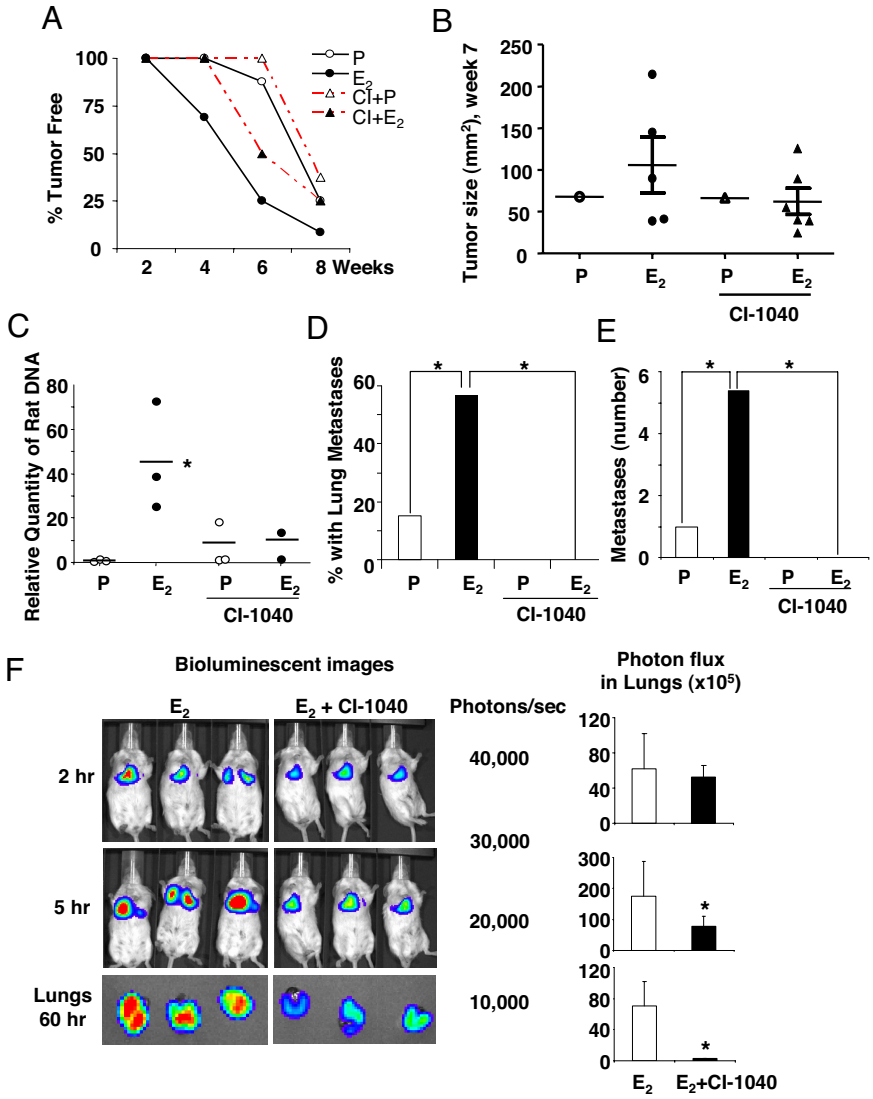

Fig. 6. The MEK1/2 inhibitor CI-1040 blocks the estrogen-driven metastasis of ELT3 cells in vivo. ELT3 cells were injected into female ovariectomized nude mice implanted with estrogen or placebo pellets. Animals were treated with CI-1040 (150 mg/kg/day by gavage, twice a day) starting 1 day post-ELT3 cell inoculation for the xenograft experiments (*A–E*), or 2 days before cell inoculation for i.v. injection (*F*). (*A*) Tumor development was recorded as the percentage of tumor-free animals post-cell inoculation. (*B*) The primary tumor area was calculated at 7 weeks post-cell inoculation. (*C*) The level of circulating ELT3 cells was measured from blood samples of xenograft animals using rat-specific qPCR amplification. (*D*) The percentage of mice with lung metastases in the placebo and estrogen-treated groups was compared. (*E*) The number of lung metastases was scored. (*F*) ELT3-luciferase cells were injected intravenously into ovariectomized female E_2-treated ($n = 5$) and CI-1040 plus E_2-treated ($n = 5$) mice. Lung colonization was measured using bioluminescence 2 and 5 h after injection. Total photon flux/second present in the chest regions were quantified and compared between E_2 ($n = 5$) and CI-1040 plus E_2-treated ($n = 5$) animals. Lungs were dissected and imaged 60 h post-cell injection. Total photon flux/second present in ex vivo lungs were quantified and compared between E_2 ($n = 5$) and CI-1040 plus E_2-treated ($n = 5$) animals. *, $P < 0.05$, Student's *t* test.

levels of circulating tumor cells in estrogen-treated mice bearing xenograft tumors. We also found that estrogen treatment enhances the survival of intravenously injected cells in the peripheral blood. These data are of particular interest because circulating LAM cells can be detected in the blood and pleural fluid of women with LAM (35). Our data provide a rationale for the potential use of circulating cells as a quantitative and rapid biomarker of response to targeted therapy in women with LAM.

In addition to promoting the levels of ELT3 cells in the peripheral blood, as measured by real-time RT-PCR using rat-specific primers, estrogen also enhanced the survival of intravenously injected luciferase-expressing ELT3 cells within the lungs. Three hours after injection, there was significantly more bioluminescence in the chest regions of the E_2-treated animals, and by 24 h this difference was even more marked. Importantly, however, 1 h after the i.v. injection of ELT3-luciferase cells, similar levels of bioluminescence were present in the lungs of estrogen-treated and placebo-treated animals, which demonstrates that similar numbers of injected cells reach the lungs. These data suggest that E_2 promotes the survival of Tsc2-null cells within the lungs.

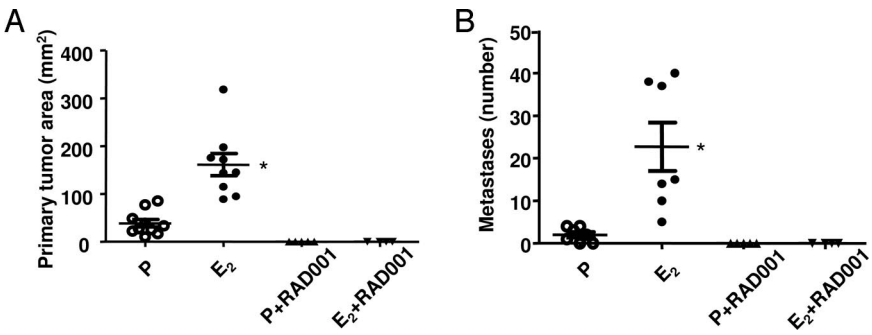

Fig. 7. The mTOR inhibitor RAD001 blocks primary tumor development and estrogen-driven metastasis of ELT3 cells in vivo. ELT3 cells were injected into female ovariectomized nude mice implanted with estrogen or placebo pellets. Animals were treated with RAD001 (4 mg/kg/day by gavage) starting 1 day post-ELT3 cell inoculation. (*A*) The primary tumor area was calculated at 8 weeks post-cell inoculation. (*B*) The number of lung metastases was scored at 8 weeks post-cell inoculation. *, $P < 0.05$, Student's *t* test.

The lack of an in vivo model of LAM has been a significant barrier in LAM research. While not a perfect surrogate, ELT3 cells have important features in common with LAM cells, including loss of Tsc2, activation of mTOR, and expression of estrogen receptor alpha and smooth muscle markers (18, 19). We are optimistic that this model of estrogen-induced metastasis will allow agents to be tested preclinically, thereby facilitating the development of therapies for LAM. Currently the only effective therapy for end-stage LAM is lung transplantation, and many women die while awaiting a donor lung or as a complication of the transplantation. There are multiple nodes that one can target in the estrogen/MEK/MAPK pathway, including inhibition of estrogen production, inhibition of the estrogen receptor, and inhibition of Raf/MEK.

Taken together, our data highlight a unique model for LAM pathogenesis in which activation of MEK by estrogen promotes the survival of detached tuberin-null cells. It will be important to confirm these findings using patient-derived cells, although this will be challenging because of the difficulties in establishing cultures of LAM cells. An alternative would be to measure levels of circulating LAM cells in women receiving hormonal therapy in the context of a clinical trial. If our model is correct, then important effects of estrogen on LAM pathogenesis may occur before the LAM cells reach the lungs and/or within the first hours of their reaching the lungs. Therefore, targeting estrogen signaling may have a major role in the treatment of early-stage LAM and/or in the prevention of LAM in women with TSC.

Methods

ELT-3 cells are Eker rat uterine leiomyoma-derived smooth muscle cells and were used in all in vitro and in vivo studies. For in vivo studies, female ovariectomized CB17-*SCID* mice were implanted with 17-beta estradiol or placebo pellets (2.5 mg, 90-day release) 1 week prior to cell inoculation. For xenograft tumor establishment, 2×10^6 ELT3 cells were bilaterally injected into the rear flanks of the mice. For intravenous injections, 2×10^5 ELT3 or ELT3-Luc cells were injected into the lateral tail vein. Lung metastases were scored from 5-micron H&E-stained sections of each lobe. CI-1040 (150 mg/kg day by gavage, twice per day) or RAD001 (4 mg/kg per day by gavage) was initiated 1 day after cell inoculation. To detect circulating ELT3 cells, 0.5 mL of mouse blood was collected by intraocular bleed, red blood cells were lysed, and genomic DNA was extracted. At death, lungs were dissected for DNA extraction. The assay for rat DNA was adapted from the method described by Walker *et al*. (36). Bioluminescent reporter imaging was performed to monitor the lung seeding of ELT3-Luciferase cells. Ten minutes prior to imaging, animals were injected with luciferin (Xenogen) (120 mg/kg, i.p.). Bioluminescent signals were recorded at indicated times post-cell injection using the Xenogen IVIS System. Total photon flux at the chest regions and from the dissected lungs was analyzed. For anoikis studies, ELT3 cells with or without 10 nM E_2 pretreatment were plated onto poly-hydroxyethyl methacrylate (PolyHEMA) culture dishes. Cell death as a function of DNA fragmentation was detected using Cell Death Detection ELISA kit (Roche Diagnostics). Full methods are available in *SI Text*.

ACKNOWLEDGMENTS. We thank Anthony Lerro for assistance in the animal studies, the Fox Chase Cancer Center Histopathology Facility for specimen preparation, Novartis for providing RAD001, and Pfizer for providing CI-1040. We are grateful to Jessica Goldhirsh and to Drs. E. Golemis and J. Chernoff for their critical reading of this manuscript. This research was funded by grants from The Adler Foundation, the LAM Treatment Alliance, the LAM Foundation, and the National Heart, Lung and Blood Institute.

1. Sullivan EJ (1998) Lymphangioleiomyomatosis: review. *Chest* 114:1689–1703.
2. Costello LC, Hartman TE, Ryu JH (2000) High frequency of pulmonary lymphangioleiomyomatosis in women with tuberous sclerosis complex. *Mayo Clin Proc* 75:591–594.
3. Franz DN, *et al.* (2001) Mutational and radiographic analysis of pulmonary disease consistent with lymphangioleiomyomatosis and micronodular pneumocyte hyperplasia in women with tuberous sclerosis. *Am J Respir Crit Care Med* 164:661–668.
4. Shepherd CW, Gomez MR, Lie JT, Crowson CS (1991) Causes of death in patients with tuberous sclerosis. *Mayo Clin Proc* 66:792–796.
5. Yu J, Astrinidis A, Henske EP (2001) Chromosome 16 loss of heterozygosity in tuberous sclerosis and sporadic lymphangiomyomatosis. *Am J Respir Crit Care Med* 164:1537–1540.
6. Plank TL, Yeung RS, Henske EP (1998) Hamartin, the product of the tuberous sclerosis 1 (TSC1) gene, interacts with tuberin and appears to be localized to cytoplasmic vesicles. *Cancer Res* 58:4766–4770.
7. van Slegtenhorst M, *et al.* (1998) Interaction between hamartin and tuberin, the TSC1 and TSC2 gene products. *Hum Mol Genet* 7:1053–1057.
8. Crino PB, Nathanson KL, Henske EP (2006) The tuberous sclerosis complex. *N Engl J Med* 355:1345–1356.
9. El-Hashemite N, Zhang H, Henske EP, Kwiatkowski DJ (2003) Mutation in TSC2 and activation of mammalian target of rapamycin signalling pathway in renal angiomyolipoma. *Lancet* 361:1348–1349.
10. Karbowniczek M, Yu J, Henske EP (2003) Renal angiomyolipomas from patients with sporadic lymphangiomyomatosis contain both neoplastic and non-neoplastic vascular structures. *Am J Pathol* 162:491–500.
11. Yu J, Astrinidis A, Howard S, Henske EP (2004) Estradiol and tamoxifen stimulate LAM-associated angiomyolipoma cell growth and activate both genomic and non-genomic signaling pathways. *Am J Physiol Lung Cell Mol Physiol* 286:L694–700.
12. Im E, *et al.* (2002) Rheb is in a high activation state and inhibits B-Raf kinase in mammalian cells. *Oncogene* 21:6356–6365.
13. Karbowniczek M, *et al.* (2004) Regulation of B-Raf kinase activity by tuberin and Rheb is mammalian target of rapamycin (mTOR)-independent. *J Biol Chem* 279:29930–29937.
14. Karbowniczek M, Robertson GP, Henske EP (2006) Rheb inhibits C-raf activity and B-raf/C-raf heterodimerization. *J Biol Chem* 281:25447–25456.
15. Carsillo T, Astrinidis A, Henske EP (2000) Mutations in the tuberous sclerosis complex gene TSC2 are a cause of sporadic pulmonary lymphangioleiomyomatosis. *Proc Natl Acad Sci USA* 97:6085–6090.
16. Karbowniczek M, *et al.* (2003) Recurrent lymphangiomyomatosis after transplantation: genetic analyses reveal a metastatic mechanism. *Am J Respir Crit Care Med* 167:976–982.
17. Logginidou H, Ao X, Russo I, Henske EP (2000) Frequent estrogen and progesterone receptor immunoreactivity in renal angiomyolipomas from women with pulmonary lymphangioleiomyomatosis. *Chest* 117:25–30.
18. Howe SR, *et al.* (1995) Rodent model of reproductive tract leiomyomata. Establishment and characterization of tumor-derived cell lines. *Am J Pathol* 146:1568–1579.
19. Howe SR, Gottardis MM, Everitt JI, Walker C (1995) Estrogen stimulation and tamoxifen inhibition of leiomyoma cell growth in vitro and in vivo. *Endocrinology* 136:4996–5003.
20. Finlay GA, Hunter DS, Walker CL, Paulson KE, Fanburg BL (2003) Regulation of PDGF production and ERK activation by estrogen is associated with TSC2 gene expression. *Am J Physiol Cell Physiol* 285:C409–418.
21. Finlay GA, *et al.* (2004) Estrogen-induced smooth muscle cell growth is regulated by tuberin and associated with altered activation of platelet-derived growth factor receptor-beta and ERK-1/2. *J Biol Chem* 279:23114–23122.
22. Pratt MA, Satkunaratnam A, Novosad DM (1998) Estrogen activates raf-1 kinase and induces expression of egr-1 in MCF-7 breast cancer cells. *Mol Cell Biochem* 189:119–125.
23. Reginato MJ, *et al.* (2003) Integrins and EGFR coordinately regulate the pro-apoptotic protein Bim to prevent anoikis. *Nat Cell Biol* 5:733–740.
24. Rytomaa M, Martins LM, Downward J (1999) Involvement of FADD and caspase-8 signalling in detachment-induced apoptosis. *Curr Biol* 9:1043–1046.
25. Schulze A, Lehmann K, Jefferies HB, McMahon M, Downward J (2001) Analysis of the transcriptional program induced by Raf in epithelial cells. *Genes Dev* 15:981–994.
26. Hanahan D, Weinberg RA (2000) The hallmarks of cancer. *Cell* 100:57–70.
27. Eckert LB, *et al.* (2004) Involvement of Ras activation in human breast cancer cell signaling, invasion, and anoikis. *Cancer Res* 64:4585–4592.
28. Tan TT, *et al.* (2005) Key roles of BIM-driven apoptosis in epithelial tumors and rational chemotherapy. *Cancer Cell* 7:227–238.
29. Sebolt-Leopold JS, *et al.* (1999) Blockade of the MAP kinase pathway suppresses growth of colon tumors in vivo. *Nat Med* 5:810–816.
30. El-Hashemite N, Walker V, Kwiatkowski DJ (2005) Estrogen enhances whereas tamoxifen retards development of Tsc mouse liver hemangioma: a tumor related to renal angiomyolipoma and pulmonary lymphangioleiomyomatosis. *Cancer Res* 65:2474–2481.
31. Migliaccio A, *et al.* (1996) Tyrosine kinase/p21ras/MAP-kinase pathway activation by estradiol-receptor complex in MCF-7 cells. *EMBO J* 15:1292–1300.
32. Razandi M, Pedram A, Park ST, Levin ER (2003) Proximal events in signaling by plasma membrane estrogen receptors. *J Biol Chem* 278:2701–2712.
33. Song RX, *et al.* (2002) Linkage of rapid estrogen action to MAPK activation by ERalpha-Shc association and Shc pathway activation. *Mol Endocrinol* 16:116–127.
34. Song RX, Zhang Z, Chen Y, Bao Y, Santen RJ (2007) Estrogen signaling via a linear pathway involving insulin-like growth factor I receptor, matrix metalloproteinases, and epidermal growth factor receptor to activate mitogen-activated protein kinase in MCF-7 breast cancer cells. *Endocrinology* 148:4091–4101.
35. Crooks DM, *et al.* (2004) Molecular and genetic analysis of disseminated neoplastic cells in lymphangioleiomyomatosis. *Proc Natl Acad Sci USA* 101:17462–17467.
36. Walker JA, *et al.* (2004) Quantitative PCR for DNA identification based on genome-specific interspersed repetitive elements. *Genomics* 83:518–527.